

# LAND COVER CLASSIFICATION OF RIVER VALLEY FOR A NEED OF HYDRODYNAMIC MODELLING OF FLOOD BASED ON AERIAL PHOTOGRAPHS AND LIDAR DATA

Przemysław Tymków<sup>1</sup>

## Abstract

Mathematic models of flood wave can be used to predict the range of flooded area. The principal aim of defining the high wave flows is to describe the characteristics of the valley like its shape and area cover. The area cover determines the resistant factor which is one of the most important parameter in hydraulic modeling. Contemporary methods of collecting and processing data give the opportunity of estimating the resistance parameter of the high wave flows on a large scale. The main aim of this research is to find a method of resistance factor identification, using remote sensing, neural networks and texture analysis. Automatic (supervised) land cover classification of a part of Widawa River valley was done using multilayer neural classifier in comparison with maximum likelihood method. As a main source of information needed for feature vector building non-metric aerial photographs were used. In order to take into account the features which describe the picture's texture, the Grey level co-occurrence matrix method (GLCM) has been used. Aerial laser scanning was used as a supplementary data source. The approach, based on integration aerial photographs taken with digital camera with LIDAR data, allows to make more detailed classification, for example which takes into consideration vegetation density below the treetop level on the forest area. In order to quantify the quality of the results in automatic manner, a confusion matrix was created for each case. As a quality parameters kappa coefficient, producer, user and overall accuracy were proposed.

## Keywords

land cover classification, neural networks, maximum likelihood, hydrodynamic modeling

## 1 INTRODUCTION

In the hydraulic modeling of the swell flows flood area properties affect many essential features like flow velocity, water level, valley capacity. The land cover and its use become very important in case of flood and should be taken into consideration during model building. Especially, while assessing the high wave flow bed capacity it is difficult to describe the parameter of lichen vegetable which determines the value of the partial resistance factor beyond the proper river bed which is component of the whole flow resistance. The value of normalized resistance factors for some standard surfaces have been put into tables (Ven Te Chow tables). The data which are essential for estimating the vegetable influence on the flow can be received directly, for instance, during the cross - section surveys or remotely, from the aerial photos, while DTM is building. Also the satellite images can be very useful and contain a lot of information. However, a wide range of investigative area disqualify the direct and remote but only manual techniques of cover estimating. To assess surface roughness factor supervised classification methods and remote sensing data have been proposed. Number of experiments have been performed to find best classification methods, which were based on different combination of features vector. The aim was to estimate the range and possibility of using aerial photographs and laser scanning data as a source of information to land cover classification of Widawa River valley. The Widawa is a river in southern Poland (Lower Silesia), a right-bank tributary of the Odra River. The study area was 10 km long and divided into three sectors: the mouth sector covered with forests, the middle, agricultural sector and the upper, partly urbanized one. The most representative results and detailed conclusions were presented in this paper.

## 2 DATA SOURCES

The automation of classification process is based on four important information taken from the teledetectical and photogrametrical sources:

- the color of single pixel (value of grey level for each RGB channel) taken from aerial photographs,
- the texture features of pictures,
- height of cover calculated on the basis of digital terrain model (DTM) and digital surface model (DSM) created by using laser scanning data
- laser intensity

---

<sup>1</sup>Przemysław Tymków, MSc Eng., Wrocław University of Environmental and Life Sciences, Faculty of Environmental Engineering and Geodesy, Institute of Geodesy and Geoinformatics, address: ul. Grunwaldzka 53 50-357 Wrocław, Poland, Phone: +48 71 3205617, email: tymkow@kgf.ar.wroc.pl

## 2.1 Aerial photographs

During laser scanning data acquisition very often non-metric photographs or video recording is taken for further interpretation. This information after calibration can be used as a reflectance data similarly to metric photogrammetrical or satellite images. Obviously the quality of this data is much worse. In this research numbers of non-metric aerial color photographs were taken with digital Nikon d70 camera. After calibration using projective transformation they were directly included into classification vector as RGB channels. The height of flight was app. 800m over terrain and the spatial resolution was app. 0.4 m. After mosaic process and resampling it was reduced to 1m. *Image Analyst's Image to Image* tool was used in this process. The RMS error of transformation was about 3-4 m. The mosaic of aerial photos is shown in the figure 1 .

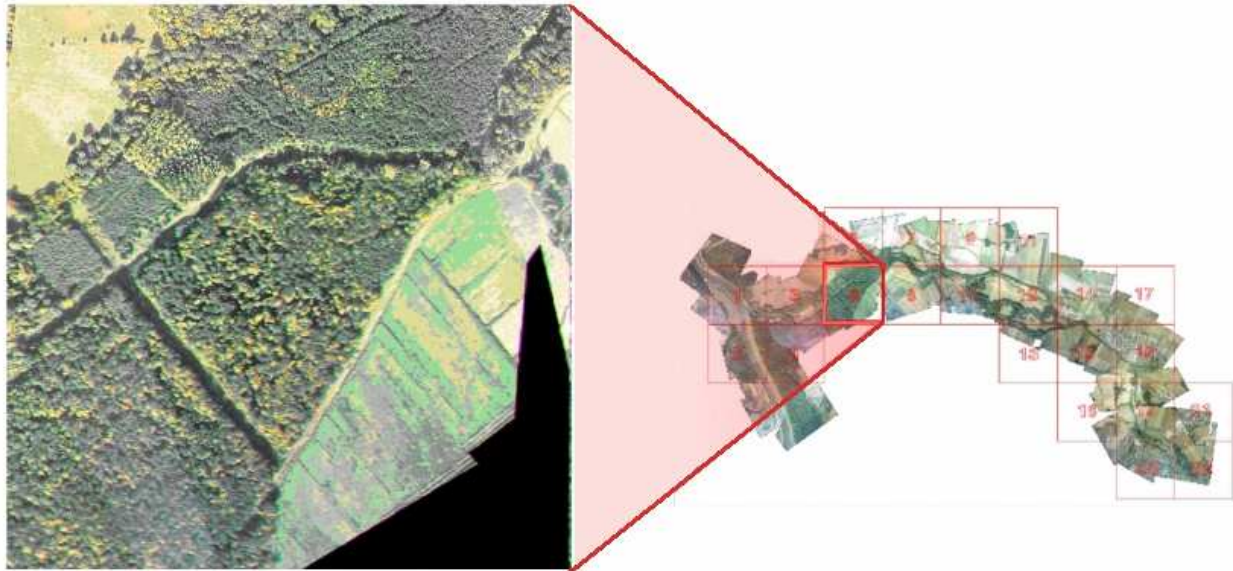


Fig. 1 Aerial photograph mosaic

## 2.2 Texture features

After calibration the aerial photographs were used to texture features extraction. The GLCM (Grey Level Co-occurrence Matrices) method was used. Grey level co-occurrence matrices estimates image properties related to second-order statistics and is one of the most well-known and widely used texture features. The entry of GLCM, which is the number of occurrences of the pair of grey levels which are a distance apart in a given direction, is defined as follows:

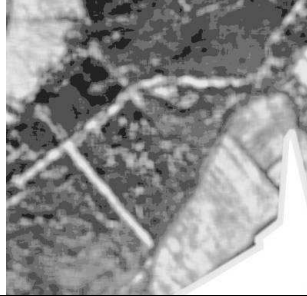
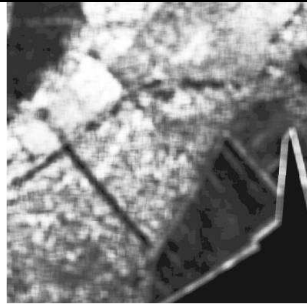
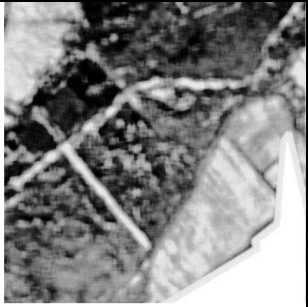
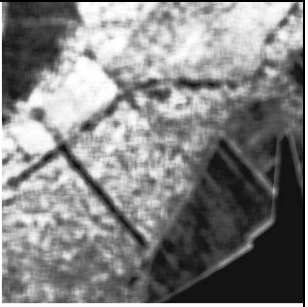
$$V_{l,\alpha}(i, j) = |\{(r, s), (t, v) : I(r, s) = i, I(t, v) = j\}| \quad (1)$$

where  $i, j = 0, \dots, N-1$ ;  $N$  – number of grey levels;  $l, \alpha$  – distance and direction angle;  $I(x, y)$  – image pixel at position  $(x, y)$ ;  $(t, v) = (r + l \cos \alpha, s + l \sin \alpha)$ . Addition of  $V_{l,\alpha}$  with its transpose divided by 2 gives symmetrical matrix  $\bar{V}_{l,\alpha}$ . Symmetrical matrix  $\bar{V}_{l,\alpha}$  might be normalized with a total number of pixels in the image before use. These transformations can be written as follows (indices  $l, \alpha$  are omitted for convenience) :

$$P_{i,j} = \frac{\bar{V}(i, j)}{\sum_{i,j=0}^{N-1} \bar{V}(i, j)}, \text{ where } \bar{V}(i, j) = \frac{V(i, j) + V^T(i, j)}{2} \quad (2)$$

The symmetrical and normalized co-occurrence matrix  $P$  reveals certain properties about the spatial distribution of the grey levels in the texture image. The definition and visualization of features used in experiments are given in table 1.

**Tab. 1** Texture features based on GLCM

ASM	energy	entropy
$\sum_{i,j=0}^{N-1} P_{i,j}^2$	$\sqrt{ASM}$	$\sum_{i,j=0}^{N-1} P_{i,j}  i-j $
		
contrast	homogeneity	dissimilarity
$\sum_{i,j=0}^{N-1} P_{i,j} (i-j)^2$	$\sum_{i,j=0}^{N-1} \frac{P_{i,j}}{1+(i-j)^2}$	$\sum_{i,j=0}^{N-1} P_{i,j}  i-j $
		

### 2.3 Laser scanning data

Laser scanning is a contemporary source of data for DTM building which very often ousts the traditional photogrammetric method. It allows to build DTM and DSM quickly, so it is a good source of information about relief. Nowadays airborne laser scanning data (points cloud) is also used for geoinformation modeling (trees, buildings, etc.). However, the direct and indirect information about terrain surface and land use contained in laser scanning data sets allow also to provide the automatic classification of land cover. On the basis of laser data two types of information were gained:

- differential model of height of land cover based on digital surface model (DSM) and digital terrain model (DTM),
- intensity image.

This information was integrated with photographs using 1x1 m grid. The visualization of differential model of height and intensity image after integration process are shown in the figure 2 and 3.

## 3 CLASSIFICATION METHODS

### 3.1 Artificial neural network classifier

The applications of artificial neural networks for solving problems in teledetection are already well-established for some time [1][2][3][4]. The networks applied were a feed-forward, multi-layer ones trained by means of Standard Back-propagation method using hand-crafted reference data. The computer software used for modeling and training neural networks was SNNS (Stuttgart Neural Network Simulator) in Linux environment. Neural classifier consists in number of neurons combined together. The input layer size is determined by the feature vector size and the output layer by the number of classes. The architecture of hidden layer has got influence on classification result. The topology of network which would optimally resolve classification problem was found through experiments.

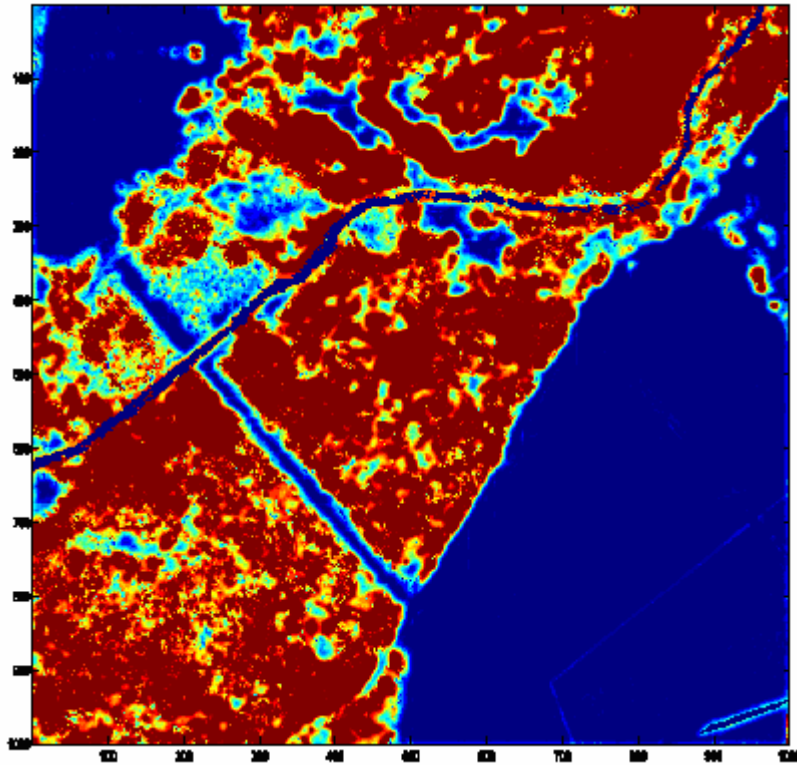


*Fig. 2 The visualization of differential model of height*

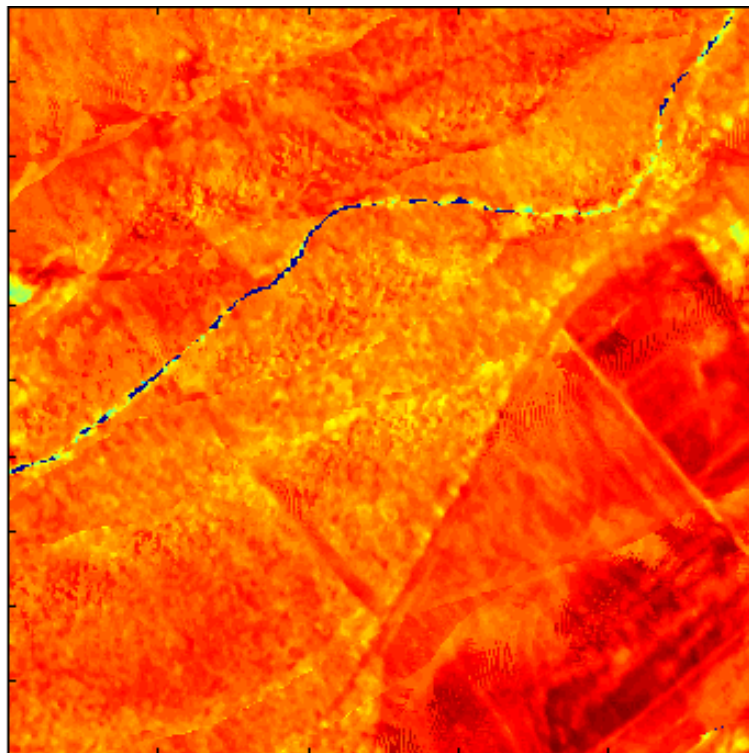


*Fig. 3 The visualization of intensity image*

Single neuron works as follow: input signals  $x_0 \dots x_n$  are multiplied by weight  $w_0 \dots w_n$ . Afterwards, the sum of this product is transformed with activation function and result of this operation is transmitted to the neurons on the next layer:

$$y(t) = f\left(\sum_{i=0}^n \omega_i(t)x_i(t)\right). \quad (3)$$

During network training, the teacher evaluates whether the output is correct. The neural weightings are reinforced or diminished depending on output correctness. An example of artificial neural network scheme used in this project is shown in figure 4.

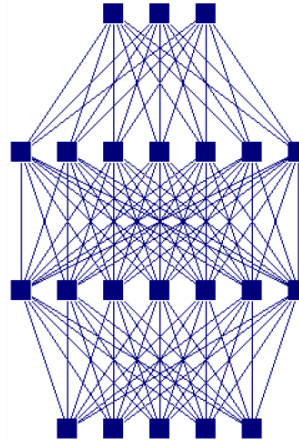


Fig. 4 An example of artificial neural network scheme

### 3.2 Maximum likelihood method

Maximum likelihood classifier also called Bayes method combines probability model with a decision rule. Usually the rule is specified as the choice of hypothesis which is the most probable. This rule is called maximum a posteriori rule. Corresponding classifier is defined by the function  $\psi^*$ :

$$\Psi^*(x) = i = p_i f_i(x) = \max_{k \in M} (p_k f_k(x)) \quad (4)$$

where:  $x = [x_1 \dots x_n]$  – vector of features,  $k$  – label of class,  $p_k$  – probability, that observed case belongs to the class  $k$  (*a priori* probability) and  $f_k$  – density function which can be approximated by the multidimensional normal distributions:

$$f_j(x) = \frac{1}{(2\pi)^{k/2} |E_j|^{1/2}} \exp\left[-0.5(x - m_j)^T E_j^{-1} (x - m_j)\right] \quad (5)$$

where:  $m_j$  – mean value vector,  $E_j$  – feature covariance matrix.

Approximation of *a priori* probability is given by:

$$\tilde{p}_j = \frac{N_j}{N}, j \in M \quad (6)$$

where:  $N_j$  – number of objects from class  $j$ ,  $N$  – number of all objects.

## 4 QUALITY MEASURES

To quantify the quality of the results a confusion matrix  $A = [a_{ij}]$  was created for each case. Element of matrix,  $a_{ij}$ , was a number of sample pixels from the  $j$ -th class that have been classified as belonging to the  $i$ -th class. On the base of matrix  $A$  the following measures have been proposed [5][6][7]:

- user's accuracy of class  $i$ :

$$u_i = \frac{a_{ii}}{a_{ri}}, \text{ where } a_{ri} = \sum_i a_{ri} \text{ (sum of } i\text{th row entries);} \quad (7)$$

- producers accuracy of class  $i$ :

$$p_i = \frac{a_{ii}}{a_{ci}}, \text{ where } a_{ci} = \sum_i a_{ci} \text{ (sum of } i\text{th column entries);} \quad (8)$$

- overall accuracy of the method:

$$d = \frac{a_{ii}}{a_t}, \text{ where } a_t \text{ is the total number of pixels;} \quad (9)$$

- Kappa coefficient:

$$\kappa = \frac{P_o - P_e}{1 - P_e}, \text{ where } P_o = \sum_i a_{ii} / a_t, \quad P_e = \sum_i a_{ri} a_{ci} / a_t^2; \quad (10)$$

The interpretation of  $\kappa$  coefficient is presented in [8]:

$0.75 \leq \kappa$  strong coincidence

$0.4 \leq \kappa < 0.75$  good enough coincidence

$\kappa < 0.40$  weak coincidence

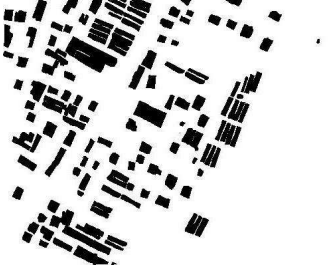
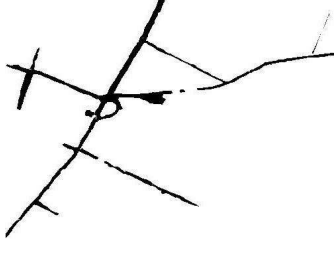
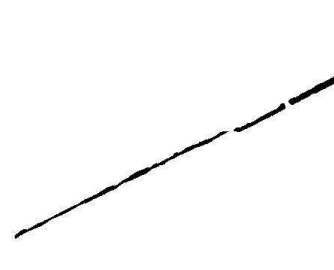
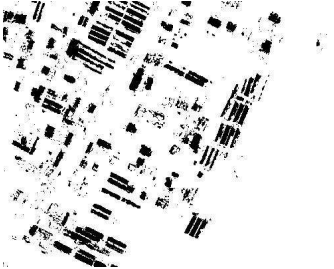
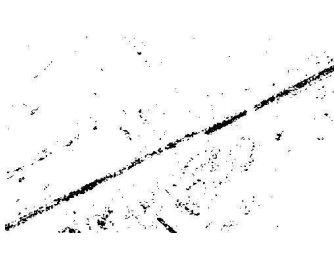
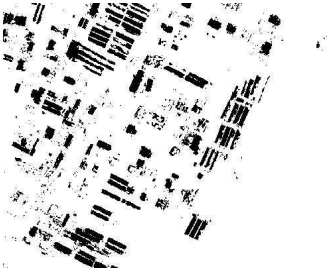
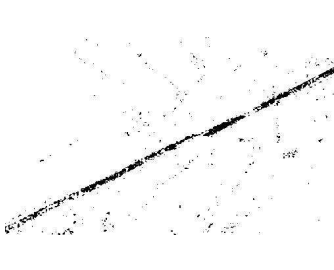
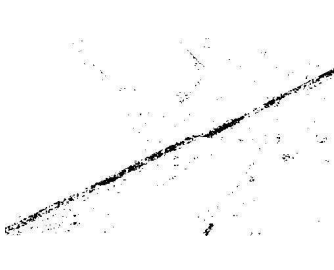
## 5 EXPERIMENTS

The first step was to find the best parameter of GLCM mask size. Four sizes of masks were tested: 7x7, 15x15, 25x25 and 35x35m in terrain. As a classifier neural network with two hidden layer of nine neurons was used in this task. Number of experiments were performed, the results of classification were visualized and quality measure was calculated. This allowed to find the best size of GLCM mask for each class. The quality parameters of all classes are presented in table 3. With bolded font the best size for each class was marked. An example of visualization of training sets for classes: buildings, roads and railway is shown in table 3.

**Tab. 2** Quality measure of classification of testing sets for classes: buildings, roads, railway and different GLCM masks sizes

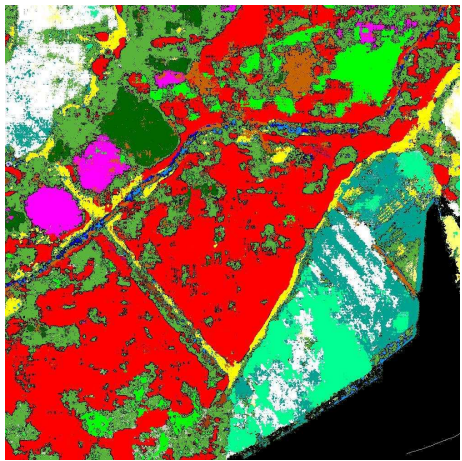
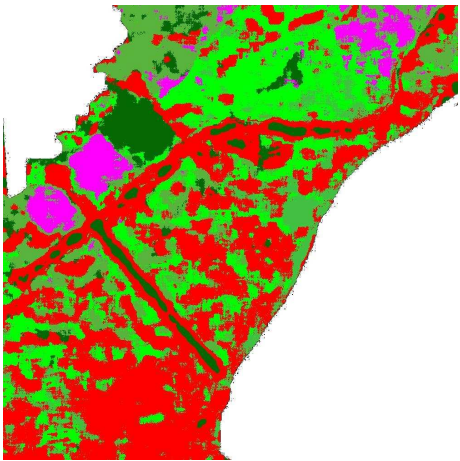
Class	Mask size	Quality measure			
		$p_i$	$u_i$	$d$	$\kappa$
Buildings	<b>7x7</b>	<b>0.74475</b>	<b>0.85360</b>	<b>0.69286</b>	<b>0.96251</b>
	15x15	0.93114	0.99120	0.88721	0.99037
	25x25	0.99114	0.98800	0.99557	0.99883
	35x35	0.99265	0.98880	0.99758	0.99903
Roads	<b>7x7</b>	<b>0.95023</b>	<b>0.95800</b>	<b>0.94964</b>	<b>0.99337</b>
	15x15	0.83351	0.95600	0.75994	0.97529
	25x25	0.62491	0.71480	0.60270	0.94597
	35x35	0.72275	0.90920	0.63262	0.95580
Railway	<b>7x7</b>	<b>0.82642</b>	<b>0.76000</b>	<b>0.93274</b>	<b>0.97894</b>
	15x15	0.71512	0.64160	0.85365	0.96654
	25x25	0.57326	0.46320	0.83190	0.95497
	35x35	0.56534	0.59200	0.60041	0.94271
Oak forest	7x7	0.75079	0.71480	0.82808	0.96903
	15x15	0.97015	0.95240	0.99291	0.99611
	25x25	0.97530	0.97080	0.98339	0.99674
	<b>35x35</b>	<b>1.00000</b>	<b>1.00000</b>	<b>1.00000</b>	<b>1.00000</b>
Meadow	7x7	0.13088	0.12400	0.27003	0.91349
	15x15	0.01956	0.02440	0.13319	0.91897
	<b>25x25</b>	<b>0.25722</b>	<b>0.16480</b>	<b>0.82731</b>	<b>0.93789</b>
	35x35	0.03007	0.02040	0.32075	0.92694
Meadow with shrubbery	7x7	0.65547	0.75280	0.62401	0.94994
	<b>15x15</b>	<b>0.73433</b>	<b>0.74080</b>	<b>0.76561</b>	<b>0.96529</b>
	25x25	0.64557	0.75360	0.60892	0.94783
	35x35	0.66457	0.72800	0.65538	0.95323
Flow water	<b>7x7</b>	<b>0.97355</b>	<b>0.98560</b>	<b>0.96552</b>	<b>0.99646</b>
	15x15	0.83626	0.99840	0.73956	0.97477
	25x25	0.78961	0.96120	0.69551	0.96717
	35x35	0.80848	0.98080	0.71093	0.97014

**Tab. 3** Classification of testing sets for classes: buildings, roads, railway and different GLCM masks sizes

	buildings	roads	railway
Aerial image			
Reference image			
Mask 7x7			
Mask 15x15			
Mask 25x25			
Mask 35x35			

In the second series of experiments classifiers have been built and trained to recognize and classify all classes such as forests of some type, buildings, etc. simultaneously, and then verified by processing a separate data, and comparing the results to a reference-classified testing sets. A comparison of classification obtained with artificial neural networks and maximum likelihood method is presented below. The huge drawback of the second method is that in some classes like for example roads or water the distribution of information about height of land cover can not be approximated with normal distribution. So this method is useless in this case.

**Tab. 4** A comparison of classification obtained with artificial neural networks and maximum likelihood method

Artificial neural networks	Maximum likelihood	Legend
		<ul style="list-style-type: none"> <li><span style="display: inline-block; width: 15px; height: 15px; background-color: magenta; border: 1px solid black; margin-right: 5px;"></span> Young oak forest</li> <li><span style="display: inline-block; width: 15px; height: 15px; background-color: green; border: 1px solid black; margin-right: 5px;"></span> Poplar forest</li> <li><span style="display: inline-block; width: 15px; height: 15px; background-color: red; border: 1px solid black; margin-right: 5px;"></span> Mixed forest</li> <li><span style="display: inline-block; width: 15px; height: 15px; background-color: cyan; border: 1px solid black; margin-right: 5px;"></span> Middle-aged oak forest</li> <li><span style="display: inline-block; width: 15px; height: 15px; background-color: brown; border: 1px solid black; margin-right: 5px;"></span> Willow forest</li> <li><span style="display: inline-block; width: 15px; height: 15px; background-color: yellow; border: 1px solid black; margin-right: 5px;"></span> Old Oak forest</li> <li><span style="display: inline-block; width: 15px; height: 15px; background-color: blue; border: 1px solid black; margin-right: 5px;"></span> Polder</li> <li><span style="display: inline-block; width: 15px; height: 15px; background-color: white; border: 1px solid black; margin-right: 5px;"></span> River</li> <li><span style="display: inline-block; width: 15px; height: 15px; background-color: white; border: 1px solid black; margin-right: 5px;"></span> Meadow</li> <li><span style="display: inline-block; width: 15px; height: 15px; background-color: lightgreen; border: 1px solid black; margin-right: 5px;"></span> Meadow with shrubbery</li> </ul>

**Tab. 5** A comparison of classification obtained with artificial neural networks and maximum likelihood method

Class	Artificial neural networks				Maximum likelihood			
	$p_i$	$u_i$	d	$\kappa$	$p_i$	$u_i$	d	$\kappa$
Young oak forest	0.91232	0.78817	0.48089	0.54300	0.58400	0.74149	0.42696	0.52247
Poplar forest	0.99587	0.81318			0.90600	0.76962		
Mixed forest	0.36467	0.19749			0.54320	0.54363		
Middle-aged oak forest	0.41935	0.37919			0.34760	0.51787		
Birch forest	0.51227	0.83265			0.71080	0.36399		
Old Oak forest	0.74847	0.85889			0.04320	0.10485		
Polder	0.9961	0.9899			-	-		
River	0.9608	0.9570			-	-		
Meadow	0.9991	0.9948			-	-		
Meadow with shrubbery	0.7848	0.7210			-	-		

## 6 CONCLUSION

The conception of using modern techniques of getting and processing digital data for hydraulic modeling presented above is a contemporary tendency of interdisciplinary problem solution. It enables the use of automatic transformation of the estimated factors into the contemporary modeling systems. The connection of teledetecion, computer science and hydraulics can be a basis for an appreciable progress in the methodology of elaborating the swell flow models, especially if the range of using them as well as the processing of time and monitoring of changes in the valleys are concerned for taking them into account in the model.

Experiments and obtained results prove that integrated RGB, GLCM and LIDAR data can be classified automatically by supervised learning with a neural network or maximum likelihood algorithm. In some cases the results are very good, such as class buildings, and in some cases only barely acceptable like roads. However, including information about height (differential model or variance of height) in classification vector along with RGB and texture features reduces errors (for example caused by the imperfection of tone equalization). The GLCM mask size should be selected for each class. Artificial neural networks gives usually better results then Bayes algorithm. Also can be used to classify data without normal distribution. The aforementioned method of area classification for a need of hydrodynamic roughness identification is in wider scope perspective for such studies, hence there is a constant need to improve it in order to achieve better results.

### Literature

- [1] LIU X.-H., SKIDMORE A., VAN OOSTEN H., *Integration of classification methods for improvement of land-cover map accuracy*. ISPRS Journal of Photogrammetry and Remote Sensing, 56(4), 2002, p.257–268.
- [2] GERMAN G. W. H., GAHEGAN M. N., *Neural network architectures for the classification of temporal image sequences*. Computers and Geosciences, 22(9), 1996, p.969–979.
- [3] MILLER D. M., KAMINSKY E. J., RANA S., *Neural network classification of remote-sensing data*. Computers and Geosciences, 21(3), 1995, p.377–386.
- [4] RUIZ-DEL SOLAR J., *TEXSOM: Texture segmentation using self-organizing maps*. Neurocomputing, 21, 1998, p.7–18.
- [5] COHEN, J., *A Coefficient of Agreement for Nominal Scales*. Educational and Psychological Measurement, 20, 1960, p.37-46.
- [6] COHEN, J., *Weighted kappa: nominal scale agreement with provision for scale disagreement or partial credit*. Psychol. Bull., 70, 1968, p.213-220.
- [7] HUBERT-MOY, L., COTONNEC, A., DU, L.L., CHARDIN, A., PEREZ, P., *A Comparison of Parametric Classification Procedures of Remotely Sensed Data Applied on Different Landscape Units*. Remote Sensing of Environment, 75(2), 2001, p. 174-187.
- [8] FLEISS J. L., *Statistical Methods for Rates and Proportions*, volume 20 John Wiley & Sons, New York, second edition , 1981.

### Reviewer

Andrzej Borkowski, Ph.D., D.Sc., borkowski@kgf.ar.wroc.pl, Wrocław University of Environmental and Life Sciences, The Faculty of Environmental Engineering and Geodesy, Institute of Geodesy and Geoinformatics, Grunwaldzka 53, 50-357 Wrocław, Poland